Sensitivity to SUSY Seesaw Parameters and Lepton Flavour Violation

A. M. Teixeira
Laboratoire de Physique Théorique, UMR 8627, Université de Paris-Sud XI, Bâtiment 201, F-91405 Orsay Cedex, France
S. Antusch, E. Arganda, M. J. Herrero
Departamento de Física Teórica C-XI and Instituto de Física Teórica C-XVI, Universidad Autónoma de Madrid, Cantoblanco, E-28049 Madrid, Spain

We address the constraints on the SUSY seesaw parameters arising from Lepton Flavour Violation observables. Working in the Constrained Minimal Supersymmetric Standard Model extended by three right-handed (s)neutrinos, we study the predictions for the branching ratios of $l_j \to l_i\,\gamma$ and $l_j \to 3\,l_i$ channels. We impose compatibility with neutrino data, electric dipole moment bounds, and further require a successful baryon asymmetry of the Universe (via thermal leptogenesis). We emphasise the interesting interplay between θ_{13} and the LFV muon decays, pointing out the hints on the SUSY seesaw parameters that can arise from measurements of θ_{13} and LFV branching ratios. This is a brief summary of the work of Ref. [1].

1. Introduction

Supersymmetric (SUSY) extensions of the Standard Model (SM), including three right-handed neutrino superfields, are well motivated models which can accommodate a seesaw mechanism [2], and at the same time stabilise the hierarchy between the scale of new physics and the electroweak (EW) scale. One of the most striking phenomenological implications of SUSY seesaw models is the prediction of sizable rates for lepton flavour violating (LFV) processes [3], many orders of magnitude larger than those expected from the SM seesaw. In this sense, the $l_j \to l_i\,\gamma$ and $l_j \to 3\,l_i$ ($i \neq j$) lepton decay channels, as well as $\mu - e$ conversion in heavy nuclei, are among the most interesting processes. Experimentally, the most promising decay is the $\mu \to e\,\gamma$ process, which exhibits the most stringent present bounds, and offers a significant improvement regarding the future sensitivity.

Given the fact that both light and heavy neutrinos enter in the determination of the LFV rates (via the Yukawa interactions), a powerful link between the low- and high-energy neutrino parameters can be obtained from these LFV processes. From the requirement of compatibility with current LFV bounds and with low-energy neutrino data, one can then extract information on the heavy neutrino sector, thus providing an indirect access to the heavy neutrino parameters.

In Ref. [1], we have systematically explored the sensitivity of LFV processes to θ_{13} in a broad class of SUSY seesaw scenarios, with different possibilities for the mixing in the neutrino sector. We have also incorporated in our analysis the requirement of generating a successful baryon asymmetry of the Universe (BAU) via thermal leptogenesis [4]. In particular, we have shown that various of the $l_j \to l_i\,\gamma$ and $l_j \to 3\,l_i$ ($i \neq j$) channels indeed offer interesting expectations regarding the sensitivity to θ_{13}. This sensitivity to θ_{13} had been previously pointed out [5, 6], for some specific seesaw cases.

Ultimately, and as shown in [1], the impact of a potential θ_{13} measurement on the LFV branching ratios, together with the current and future experimental bounds (measurements) on the latter ratios, may lead to a better knowledge (determination) of the heavy neutrino parameters.

2. LFV within the SUSY Seesaw

The leptonic superpotential containing the relevant terms to describe a type-I SUSY seesaw is given by $W = \hat{N}^c Y_\nu \hat{L} \hat{H}_2 + \hat{E}^c Y_l \hat{L} \hat{H}_1 + \frac{1}{2} \hat{N}^c m_N \hat{N}^c$, where $\hat{N}^c$ is the additional superfield that contains the right-handed neutrinos and their scalar partners, $Y_{l,\nu}$ are the lepton Yukawa couplings and m_N is Majorana mass. Henceforth we will assume that we are in a basis where Y_l and m_M are diagonal in flavour space. After EW symmetry breaking, the full 6×6 neutrino mass matrix is given in terms of the 3×3 Majorana mass matrix m_N, and the 3×3 Dirac mass matrix $m_D = Y_\nu v_2$, where Y_ν denotes the neutrino Yukawa couplings and $v_{1(2)}$ are the vacuum expectation values of the neutral Higgs scalars, with $v_{1(2)} = v \cos(\sin)\beta$ ($v = 174$ GeV).

In the seesaw limit, $v \ll m_N$, we obtain the seesaw equation for the light neutrino masses, $m_\nu = -m_D^T m_M^{-1} m_D$. The diagonalisation of the full neutrino mass matrix leads to the six physical Majorana states: three light ν_i and three heavy states N_i. Their masses are given by $m_\nu^{\text{diag}} = U_{\text{MNS}}^T m_\nu U_{\text{MNS}} = \text{diag}\,(m_{\nu_1}, m_{\nu_2}, m_{\nu_3})$ and $m_N^{\text{diag}} = \text{diag}\,(m_{N_1}, m_{N_2}, m_{N_3})$. We use the standard parameterisation for the Maki-Nakagawa-Sakata unitary matrix U_{MNS} [7], in terms of three mixing angles θ_{12}, θ_{23} and θ_{13}, and three CP violating phases, δ, ϕ_1 and ϕ_2.

Following the parameterisation proposed in [8], the solution to the seesaw equation can be written as

$$m_D = i \sqrt{m_N^{\text{diag}}}\, R \sqrt{m_\nu^{\text{diag}}}\, U_{\text{MNS}}^\dagger \,, \qquad (1)$$

where R is a generic complex orthogonal 3×3 matrix, defined by three complex angles θ_i. This parameterisation allows to accommodate the experimental data, while leaving room for extra neutrino mixings, in addition to those in U_{MNS}. It further shows how large Yukawa couplings $Y_\nu \sim \mathcal{O}(1)$ can be obtained by choosing large entries in m_N^{diag}.

In our analysis, we have considered scenarios of hierarchical heavy and light neutrinos, $m_{N_1} \ll m_{N_2} \ll m_{N_3}$ and $m_{\nu_1} \ll m_{\nu_2} \ll m_{\nu_3}$, with $m_{\nu_2}^2 = \Delta m_{\mathrm{sol}}^2 + m_{\nu_1}^2$ and $m_{\nu_3}^2 = \Delta m_{\mathrm{atm}}^2 + m_{\nu_1}^2$. Regarding the numerical estimates, we have used $\Delta m_{\mathrm{sol}}^2 = 8 \times 10^{-5} \mathrm{eV}^2$, $\Delta m_{\mathrm{atm}}^2 = 2.5 \times 10^{-3} \mathrm{eV}^2$, $\theta_{12} = 30°$, $\theta_{23} = 45°$, $\theta_{13} \lesssim 10°$. For simplicity we have further set $\delta = \phi_1 = \phi_2 = 0$.

Within the context of the Constrained Minimal Supersymmetric Standard Model (CMSSM), universality of the soft SUSY breaking parameters is imposed at a high-energy scale M_X, which we choose to be the $SU(2) - U(1)$ gauge coupling unification scale ($M_X \approx 2 \times 10^{16}$ GeV). Instead of scanning over the full CMSSM parameter space (generated by $M_{1/2}$, M_0, A_0, $\tan\beta$, $\mathrm{sign}\mu$), we considered specific choices for the latter parameters, given by some of the "Snowmass Points and Slopes" (SPS) [9] cases defined in Table I.

Table I Values of $M_{1/2}$, M_0, A_0, $\tan\beta$, and $\mathrm{sign}(\mu)$ for the SPS points considered in the analysis.

SPS	$M_{1/2}$ (GeV)	M_0 (GeV)	A_0 (GeV)	$\tan\beta$	μ
1 a	250	100	-100	10	> 0
1 b	400	200	0	30	> 0
2	300	1450	0	10	> 0
3	400	90	0	10	> 0
4	300	400	0	50	> 0
5	300	150	-1000	5	> 0

Regarding our computation of the LFV observables [1], it is important to stress the following points:

- It is a full one-loop computation of the branching ratios (BRs), i.e., we include all contributing one-loop diagrams with the SUSY particles flowing in the loops. For the case of $l_j \rightarrow l_i\gamma$, the analytical formulae can be found in [6, 10]. Regarding the $l_j \rightarrow 3l_i$ decays, the complete set of diagrams (including photon-penguin, Z-penguin, Higgs-penguin and box diagrams) and formulae are given in [6].

- The computation is performed in the physical basis for all SUSY particles entering in the loops. In other words, we do not use the Mass Insertion Approximation (MIA).

- To obtain the low-energy parameters of the model the full renormalisation group equations

(RGEs), including relevant terms and equations for the neutrinos and sneutrinos, are firstly run down from M_X to m_N. At the seesaw scale (in particular at m_{N_3}), we impose the boundary condition of Eq. (1). After the decoupling of the heavy neutrinos and sneutrinos, the new RGEs are then run down from m_{N_1} to the EW scale, at which the observables are computed. More concretely, we do not use the Leading Log Approximation (LLog), but rather numerically solve the full one-loop RGEs.

- The numerical implementation of the above procedure is achieved by means of the public Fortran code `SPheno2.2.2` [11], which has been adapted in order to fully incorporate the right-handed neutrino (and sneutrino) sectors, as well as the full lepton flavour structure [6].

- The SPheno code has been further enlarged by additional subroutines that compute the LFV branching ratios for all the $l_j \rightarrow l_i\gamma$ and $l_j \rightarrow 3l_i$ channels [6]. We have also included subroutines [1] to implement the requirement of successful baryogenesis (which we define as having $n_B/n_\gamma \in [10^{-10}, 10^{-9}]$) via thermal leptogenesis in the presence of upper bounds on the reheat temperature, and to ensure compatibility with present bounds on lepton electric dipole moments (EDMs): $\mathrm{EDM}_{e\mu\tau} \lesssim (6.9 \times 10^{-28}, 3.7 \times 10^{-19}, 4.5 \times 10^{-17})$ e.cm [12].

In what follows we present our main results for the case of hierarchical heavy neutrinos. We also include a comparison with present bounds on LFV rates [13, 14, 15, 16, 17] and their future sensitivities [18, 19, 20, 21] collected in Table II.

Table II Present bounds and future sensitivities for the LFV processes.

LFV process	Present bound	Future sensitivity
$\mathrm{BR}(\mu \rightarrow e\,\gamma)$	1.2×10^{-11}	1.3×10^{-13}
$\mathrm{BR}(\tau \rightarrow e\,\gamma)$	1.1×10^{-7}	10^{-8}
$\mathrm{BR}(\tau \rightarrow \mu\,\gamma)$	6.8×10^{-8}	10^{-8}
$\mathrm{BR}(\mu \rightarrow 3\,e)$	1.0×10^{-12}	10^{-13}
$\mathrm{BR}(\tau \rightarrow 3\,e)$	2.0×10^{-7}	10^{-8}
$\mathrm{BR}(\tau \rightarrow 3\,\mu)$	1.9×10^{-7}	10^{-8}

3. Results and Discussion

Here we focus on the sensitivity of the BRs to θ_{13}, and on the dependence on other relevant parameters, which, for the case of hierarchical heavy neutrinos, are the heaviest mass m_{N_3}, $\tan\beta$, θ_1 and θ_2 (using
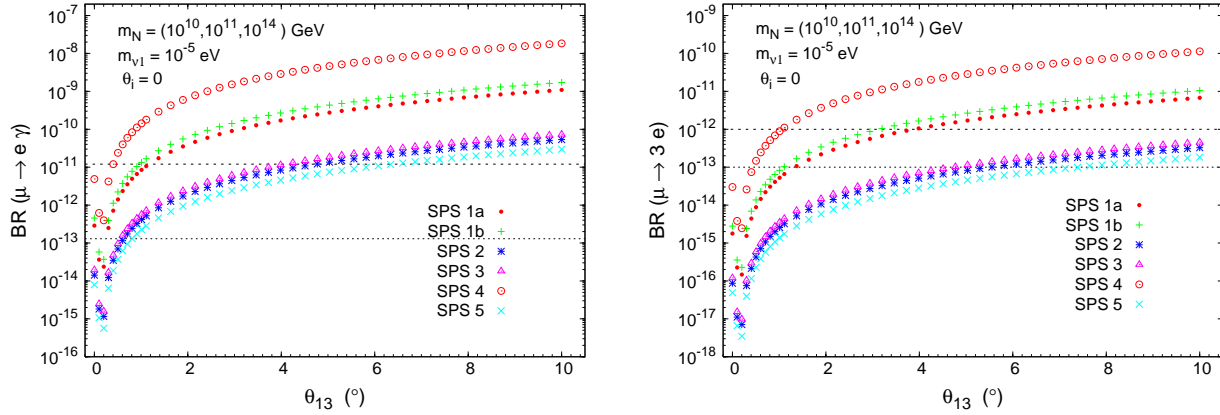
Figure 1: BR($\mu \to e\gamma$) and BR($\mu \to 3e$) as a function of θ_{13} (in degrees), for SPS 1a (dots), 1b (crosses), 2 (asterisks), 3 (triangles), 4 (circles) and 5 (times). A dashed (dotted) horizontal line denotes the present experimental bound (future sensitivity).

the R parameterisation of [8]). The other input seesaw parameters m_{N_1}, m_{N_2} and θ_3, play a secondary role since the BRs do not strongly depend on them. Finally, we comment on the hints on the SUSY seesaw parameters that can be derived from a measurement of the BRs and θ_{13}.

For $R = 1$, the predictions of the BRs as functions of θ_{13} in the experimentally allowed range of θ_{13}, $0° \leq \theta_{13} \leq 10°$ are illustrated in Fig. 1. In this figure we also include the present and future experimental sensitivities for the channels. We clearly see that the BRs of $\mu \to e\gamma$ and $\mu \to 3e$ are extremely sensitive to θ_{13}, with their predicted rates varying many orders of magnitude along the explored θ_{13} interval. The BRs of $\tau \to e\gamma$ and $\tau \to 3e$ channels are also sensitive to θ_{13}, but experimentally less challenging. The other LFV channels, $\tau \to \mu\gamma$ and $\tau \to 3\mu$, are nearly insensitive to this parameter (see [1]). In the case of $\mu \to e\gamma$ this strong sensitivity was previously pointed out in Ref. [5]. In [6], working within a full RGE approach, it was noticed that $\mu \to e\gamma$ and $\mu \to 3e$ were the channels that, in addition to manifesting a clear θ_{13} dependency, were the most promising from the experimental detection point of view.

The most important conclusion from Fig. 1 is that, for this choice of parameters, the predicted BRs for both muon decay channels, $\mu \to e\gamma$ and $\mu \to 3e$, are clearly within the present experimental reach for several of the studied SPS points. The most stringent channel is manifestly $\mu \to e\gamma$ where the predicted BRs for all the SPS points are clearly above the present experimental bound for $\theta_{13} \gtrsim 5°$. With the expected improvement in the experimental sensitivity to this channel, this would happen for $\theta_{13} \gtrsim 1°$.

In addition to the small neutrino mass generation, the seesaw mechanism offers the interesting possibility of baryogenesis via leptogenesis [4]. Thermal leptogenesis is an attractive and minimal mechanism to produce a successful BAU, even compatible with present data, $n_B/n_\gamma \approx (6.10 \pm 0.21) \times 10^{-10}$ [22]. In the supersymmetric version of the seesaw mechanism, it can be successfully implemented provided that the following conditions can be satisfied. Firstly, Big Bang Nucleosynthesis gravitino problems have to be avoided, which is possible, for instance, for sufficiently heavy gravitinos. Since we consider the gravitino mass as a free parameter, this condition can be easily achieved. In any case, further bounds on the reheat temperature, $T_{\rm RH}$, still arise from decays of gravitinos into the lightest supersymmetric particle (LSP). In the case of heavy gravitinos and neutralino LSP masses in the range 100-150 GeV (which is the case of our work), one obtains $T_{\rm RH} \lesssim 2 \times 10^{10}$ GeV. In the presence of these constraints on $T_{\rm RH}$, the favoured region by thermal leptogenesis corresponds to small (but nonvanishing) complex R-matrix angles θ_i. For vanishing $U_{\rm MNS}$ CP phases the constraints on R are basically $|\theta_2|, |\theta_3| \lesssim 1$ rad (mod π). Thermal leptogenesis also constrains m_{N_1} to be roughly in the range $[10^9 \, {\rm GeV}, 10 \times T_{\rm RH}]$ (see also [23, 24]).

In [1] we have explicitly calculated the produced BAU in the presence of upper bounds on the reheat temperature $T_{\rm RH}$. We have furthermore set as "favoured BAU values" those that are within the interval $[10^{-10}, 10^{-9}]$, which contains the WMAP value, and chosen the value of $m_{N_1} = 10^{10}$ GeV in most of our analysis. Similar studies of the constraints from leptogenesis on LFV rates have been done in [25].

For very small values of m_{ν_1} ($m_{\nu_1} \sim \mathcal{O}(10^{-5} \, {\rm eV})$) a baryon asymmetry in the range 10^{-10} to 10^{-9} can be obtained for a considerable region of the $|\theta_2|$ parameter space, with the BRs exhibiting a clear sensitivity to the value of θ_{13} [1]. On the other hand, the situation changes dramatically for larger values of m_{ν_1}.
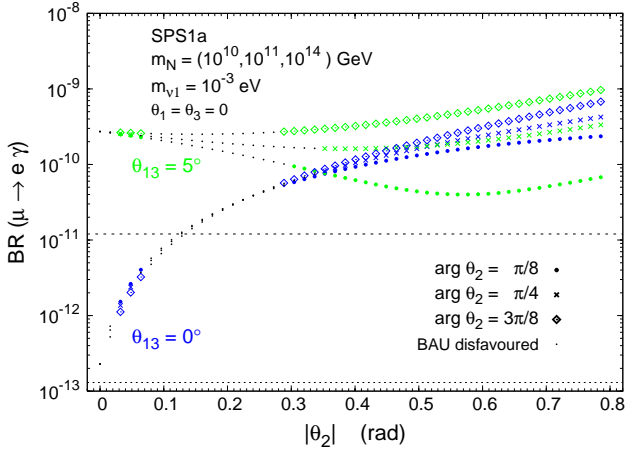
Figure 2: BR($\mu \to e\,\gamma$) as a function of $|\theta_2|$, for $\arg\theta_2 = \{\pi/8\,,\,\pi/4\,,\,3\pi/8\}$ (dots, times, diamonds, respectively) and $\theta_{13} = 0°,\,5°$ (blue/darker, green/lighter lines). We take $m_{\nu_1} = 10^{-3}$ eV. In all cases black dots represent points associated with a disfavoured BAU scenario and a dashed (dotted) horizontal line denotes the present experimental bound (future sensitivity).

Figure 3: BR($\mu \to e\,\gamma$) as a function of m_{N_3} for SPS 1a, with $m_{\nu_1} = 10^{-5}$ eV and $m_{\nu_1} = 10^{-3}$ eV (times, dots, respectively), and $\theta_{13} = 0°,\,5°$ (blue/darker, green/lighter lines). Baryogenesis is enabled by the choice $\theta_2 = 0.05\,e^{0.2\,i}$ ($\theta_1 = \theta_3 = 0$). On the upper horizontal axis we display the associated value of $(Y_\nu)_{33}$. A dashed (dotted) horizontal line denotes the present experimental bound (future sensitivity).

In Fig. 2, we display the dependence of the most sensitive BR to θ_{13}, BR($\mu \to e\,\gamma$), on $|\theta_2|$. We consider two particular values of θ_{13}, $\theta_{13} = 0°,5°$ and choose SPS 1a. Motivated from the thermal leptogenesis favoured θ_2-regions [1], we take $0 \lesssim |\theta_2| \lesssim \pi/4$, with $\arg\theta_2 = \{\pi/8\,,\,\pi/4\,,\,3\pi/8\}$. We choose $m_{\nu_1} = 10^{-3}$ eV, while for the heavy neutrino masses we take $m_N = (10^{10},\,10^{11},\,10^{14})$ GeV.

While for smaller values of $|\theta_2|$ the branching ratio displays a clear sensitivity to having θ_{13} equal or different from zero (a separation larger than two orders of magnitude for $|\theta_2| \lesssim 0.05$), the effect of θ_{13} is diluted for increasing values of $|\theta_2|$. For $|\theta_2| \gtrsim 0.3$ the BR($\mu \to e\,\gamma$) associated with $\theta_{13} = 5°$ can be even smaller than for $\theta_{13} = 0°$. This implies that in this case, a potential measurement of BR($\mu \to e\,\gamma$) would not be sensitive to θ_{13}. Similar results were obtained for θ_3, but for shortness are not shown here.

Concerning the EDMs, which are clearly non-vanishing in the presence of complex θ_i, we have checked that all the predicted values for the electron, muon and tau EDMs are well below the experimental bounds.

We now consider the dependence of BR($\mu \to e\gamma$) on m_{N_3}. As displayed in Fig. 3, there is a strong sensitivity of the BRs to m_{N_3}. In fact, the BRs vary by as much as six orders of magnitude in the explored range of 5×10^{11} GeV $\leq m_{N_3} \leq 5 \times 10^{14}$ GeV. Notice also that for the largest values of m_{N_3} considered, the predicted rates for $\mu \to e\gamma$ enter into the present experimental reach. Although not shown here, it is also worth mentioning that by comparing our full results with the LLog predictions, we found that the LLog ap-
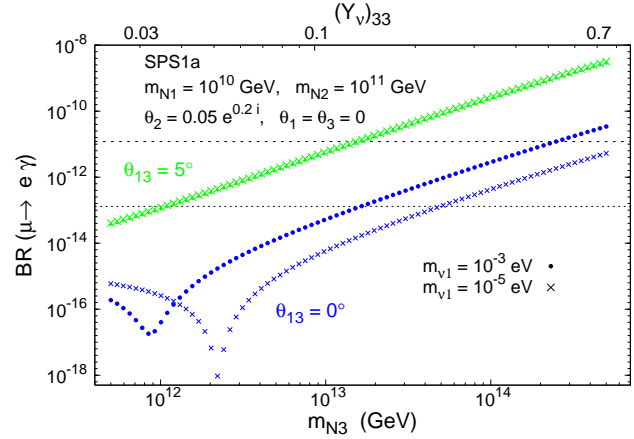
proximation dramatically fails in some cases [1]. Similar effects were also noticed in [26, 27].

Regarding the $\tan\beta$ dependence of the BRs we obtained that the BR grow as $\tan^2\beta$. In fact, the hierarchy of the BR predictions for the several SPS points (as already manifest in Fig.1) is dictated by the corresponding $\tan\beta$ value, with a secondary role being played by the given SUSY spectra. We found the following generic hierarchy: $BR_{SPS4} > BR_{SPS1b} \gtrsim BR_{SPS1a} > BR_{SPS3} \gtrsim BR_{SPS2} > BR_{SPS5}$.

Let us now address the question of whether a joint measurement of the BRs and θ_{13} can shed some light on experimentally unreachable parameters, like m_{N_3}. The expected improvement in the experimental sensitivity to the LFV ratios supports the possibility that a BR could be measured in the future, thus providing the first experimental evidence for new physics, even before its discovery at the LHC. The prospects are especially encouraging regarding $\mu \to e\,\gamma$, where the experimental sensitivity will improve by at least two orders of magnitude. Moreover, and given the impressive effort on experimental neutrino physics, a measurement of θ_{13} will likely also occur in the future [28].

Given that, as previously emphasised, $\mu \to e\,\gamma$ is very sensitive to θ_{13}, whereas this is not the case for BR($\tau \to \mu\,\gamma$), and that both BRs display the same approximate behaviour with m_{N_3} and $\tan\beta$, we have studied the correlation between these two observables. This optimises the impact of a θ_{13} measurement, since it allows to minimise the uncertainty introduced from
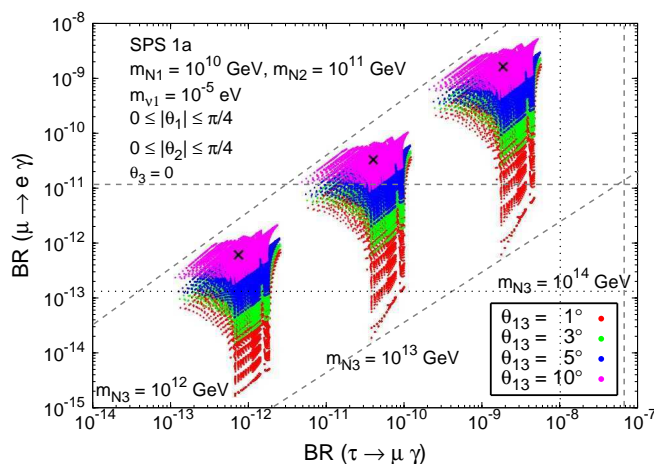
Figure 4: Correlation between $BR(\mu \to e\,\gamma)$ and $BR(\tau \to \mu\,\gamma)$ as a function of m_{N_3}, for SPS 1a. The areas displayed represent the scan over θ_i as given in Eq. (2). From bottom to top, the coloured regions correspond to $\theta_{13} = 1°$, $3°$, $5°$ and $10°$ (red, green, blue and pink, respectively). Horizontal and vertical dashed (dotted) lines denote the experimental bounds (future sensitivities).

not knowing $\tan\beta$ and m_{N_3}, and at the same time offers a better illustration of the uncertainty associated with the R-matrix angles. In this case, the correlation of the BRs with respect to m_{N_3} means that, for a fixed set of parameters, varying m_{N_3} implies that the predicted point $(BR(\tau \to \mu\,\gamma),\ BR(\mu \to e\,\gamma))$ moves along a line with approximately constant slope in the $BR(\tau \to \mu\,\gamma)$-$BR(\mu \to e\,\gamma)$ plane. On the other hand, varying θ_{13} leads to a displacement of the point along the vertical axis.

In Fig. 4, we illustrate this correlation for SPS 1a, choosing distinct values of the heaviest neutrino mass, and scanning over the BAU-enabling R-matrix angles (setting θ_3 to zero) as

$$0 \lesssim |\theta_1| \lesssim \pi/4\,, \qquad -\pi/4 \lesssim \arg\theta_1 \lesssim \pi/4\,,$$
$$0 \lesssim |\theta_2| \lesssim \pi/4\,, \qquad\quad 0 \lesssim \arg\theta_2 \lesssim \pi/4\,,$$
$$m_{N_3} = 10^{12}\,,\ 10^{13}\,,\ 10^{14}\,\mathrm{GeV}\,. \qquad (2)$$

We considered the following values, $\theta_{13} = 1°$, $3°$, $5°$ and $10°$, and only included in the plot the BR predictions which allow for a favourable BAU. Other SPS points have also been considered but they are not shown here for brevity (see [1]). We clearly observe in Fig. 4 that for a fixed value of m_{N_3}, and for a given value of θ_{13}, the dispersion arising from a θ_1 and θ_2 variation produces a small area rather than a point in the $BR(\tau \to \mu\,\gamma)$-$BR(\mu \to e\,\gamma)$ plane.

The dispersion along the $BR(\tau \to \mu\,\gamma)$ axis is of approximately one order of magnitude for all θ_{13}. In contrast, the dispersion along the $BR(\mu \to e\,\gamma)$ axis increases with decreasing θ_{13}, ranging from an order of magnitude for $\theta_{13} = 10°$, to over three orders of magnitude for the case of small θ_{13} ($1°$). From Fig. 4 we can also infer that other choices of m_{N_3} (for $\theta_{13} \in [1°, 10°]$) would lead to BR predictions which would roughly lie within the diagonal lines de-

picted in the plot. Comparing these predictions for the shaded areas along the expected diagonal "corridor", with the allowed experimental region, allows to conclude about the impact of a θ_{13} measurement on the allowed/excluded m_{N_3} values.

The most important conclusion from Fig. 4 is that for SPS 1a, and for the parameter space defined in Eq. (2), an hypothetical θ_{13} measurement larger than $1°$, together with the present experimental bound on the $BR(\mu \to e\,\gamma)$, will have the impact of excluding values of $m_{N_3} \gtrsim 10^{14}$ GeV. Moreover, with the planned MEG sensitivity, the same θ_{13} measurement can further constrain $m_{N_3} \lesssim 3 \times 10^{12}$ GeV. The impact of any other θ_{13} measurement can be analogously extracted from Fig. 4.

As a final comment let us add that, remarkably, within a particular SUSY scenario and scanning over specific θ_1 and θ_2 BAU-enabling ranges for various values of θ_{13}, the comparison of the theoretical predictions for $BR(\mu \to e\,\gamma)$ and $BR(\tau \to \mu\,\gamma)$ with the present experimental bounds allows to set θ_{13}-dependent upper bounds on m_{N_3}. Together with the indirect lower bound arising from leptogenesis considerations, this clearly provides interesting hints on the value of the seesaw parameter m_{N_3}. With the planned future sensitivities, these bounds would further improve by approximately one order of magnitude.

Ultimately, a joint measurement of the LFV branching ratios, θ_{13} and the sparticle spectrum would be a powerful tool for shedding some light on otherwise unreachable SUSY seesaw parameters. It is clear from all this study that the interplay between LFV processes and future improvement in neutrino data is challenging for the searches of new physics.

Acknowledgments

References

[1] S. Antusch, E. Arganda, M. J. Herrero and A. M. Teixeira, JHEP **0611** (2006) 090 [arXiv:hep-ph/0607263].

[2] P. Minkowski, Phys. Lett. B **67** (1977) 421; M. Gell-Mann, P. Ramond and R. Slansky, in *Complex Spinors and Unified Theories* eds. P. Van. Nieuwenhuizen and D. Z. Freedman, *Supergravity* (North-Holland, Amsterdam, 1979), p.315 [Print-80-0576 (CERN)]; T. Yanagida, in *Proceedings of the Workshop on the Unified Theory and the Baryon Number in the Universe*, eds. O. Sawada and A. Sugamoto (KEK, Tsukuba, 1979), p.95; S. L. Glashow, in *Quarks and Leptons*, eds. M. Lévy *et al.* (Plenum Press, New York, 1980), p.687; R. N. Mohapatra and G. Senjanović, Phys. Rev. Lett. **44** (1980) 912.

[3] F. Borzumati and A. Masiero, Phys. Rev. Lett. **57** (1986) 961.

[4] M. Fukugita and T. Yanagida, Phys. Lett. B **174** (1986) 45.

[5] A. Masiero, S. K. Vempati and O. Vives, New J. Phys. **6** (2004) 202 [arXiv:hep-ph/0407325].

[6] E. Arganda and M. J. Herrero, Phys. Rev. D **73** (2006) 055003 [arXiv:hep-ph/0510405].

[7] Z. Maki, M. Nakagawa and S. Sakata, Prog. Theor. Phys. **28** (1962) 870; B. Pontecorvo, Sov. Phys. JETP **6** (1957) 429 [Zh. Eksp. Teor. Fiz. **33** (1957) 549]; Sov. Phys. JETP **7** (1958) 172 [Zh. Eksp. Teor. Fiz. **34** (1957) 247].

[8] J. A. Casas and A. Ibarra, Nucl. Phys. B **618** (2001) 171 [arXiv:hep-ph/0103065].

[9] B. C. Allanach *et al.*, in *Proc. of the APS/DPF/DPB Summer Study on the Future of Particle Physics (Snowmass 2001)* ed. N. Graf, Eur. Phys. J. C **25** (2002) 113 [eConf **C010630** (2001) P125] [arXiv:hep-ph/0202233].

[10] J. Hisano, T. Moroi, K. Tobe and M. Yamaguchi, Phys. Rev. D **53** (1996) 2442 [arXiv:hep-ph/9510309].

[11] W. Porod, Comput. Phys. Commun. **153** (2003) 275 [arXiv:hep-ph/0301101].

[12] W. M. Yao *et al.* [Particle Data Group], J. Phys. G **33** (2006) 1.

[13] M. L. Brooks *et al.* [MEGA Collaboration], Phys. Rev. Lett. **83** (1999) 1521 [arXiv:hep-ex/9905013].

[14] B. Aubert *et al.* [BABAR Collaboration], Phys. Rev. Lett. **96** (2006) 041801 [arXiv:hep-ex/0508012].

[15] B. Aubert *et al.* [BABAR Collaboration], Phys. Rev. Lett. **95** (2005) 041802 [arXiv:hep-ex/0502032].

[16] U. Bellgardt *et al.* [SINDRUM Collaboration], Nucl. Phys. B **299** (1988) 1.

[17] B. Aubert *et al.* [BABAR Collaboration], Phys. Rev. Lett. **92** (2004) 121801 [arXiv:hep-ex/0312027].

[18] S. Ritt [MEGA Collaboration], on the web page http://meg.web.psi.ch/docs/talks/s_ritt/mar06_novosibirsk/ritt.ppt.

[19] A. G. Akeroyd *et al.* [SuperKEKB Physics Working Group], arXiv:hep-ex/0406071.

[20] T. Iijima, "Overview of Physics at Super B-Factory", talk given at the 6th Workshop on a Higher Luminosity B Factory, KEK, Tsukuba, Japan, November 2004.

[21] J. Aysto *et al.*, arXiv:hep-ph/0109217.

[22] D. N. Spergel *et al.*, arXiv:astro-ph/0603449.

[23] G. F. Giudice, A. Notari, M. Raidal, A. Riotto and A. Strumia, Nucl. Phys. B **685** (2004) 89 [arXiv:hep-ph/0310123].

[24] S. Antusch and A. M. Teixeira, JCAP **0702** (2007) 024 [arXiv:hep-ph/0611232].

[25] S. T. Petcov, W. Rodejohann, T. Shindou and Y. Takanishi, Nucl. Phys. B **739** (2006) 208 [arXiv:hep-ph/0510404].

[26] S. T. Petcov, S. Profumo, Y. Takanishi and C. E. Yaguna, Nucl. Phys. B **676** (2004) 453 [arXiv:hep-ph/0306195].

[27] P. H. Chankowski, J. R. Ellis, S. Pokorski, M. Raidal and K. Turzynski, Nucl. Phys. B **690** (2004) 279 [arXiv:hep-ph/0403180].

[28] E. Ables et al. [MINOS Collaboration], Fermilab-proposal-0875; G. S. Tzanakos [MINOS Collaboration], AIP Conf. Proc. 721 (2004) 179; M. Komatsu, P. Migliozzi and F. Terranova, J. Phys. G **29** (2003) 443 [arXiv:hep-ph/0210043]; P. Migliozzi and F. Terranova, Phys. Lett. B **563** (2003) 73 [arXiv:hep-ph/0302274]; P. Huber, J. Kopp, M. Lindner, M. Rolinec and W. Winter, JHEP **0605** (2006) 072 [arXiv:hep-ph/0601266]; Y. Itow *et al.*, arXiv:hep-ex/0106019; A. Blondel, A. Cervera-Villanueva, A. Donini, P. Huber, M. Mezzetto and P. Strolin, arXiv:hep-ph/0606111; P. Huber, M. Lindner, M. Rolinec and W. Winter, arXiv:hep-ph/0606119; J. Burguet-Castell, D. Casper, E. Couce, J. J. Gomez-Cadenas and P. Hernandez, Nucl. Phys. B **725** (2005) 306 [arXiv:hep-ph/0503021]; J. E. Campagne, M. Maltoni, M. Mezzetto and T. Schwetz, arXiv:hep-ph/0603172.